Microwave Emission From Dry Snow: A Comparison of Experimental and Model Results

Giovanni Macelloni, Simonetta Paloscia, Paolo Pampaloni, and Marco Tedesco

Abstract—**Field measurements of microwave emission from snow-covered soil were carried out in 1996, 1997, and 1999 on the Italian Alps using a three-frequency dual polarized microwave system. At the same time, nivological time measurements were carried out using standard methods and an electromagnetic contact probe. Collected data confirmed the possibility of separating wet from dry snow and of estimating the water equivalent of dry snow. Simulations performed by means of a model based on the dense medium radiative theory (DMRT) were able to reproduce experimental data very well.**

Index Terms—**Dense medium radiative theory (DMRT), microwave emission, snow.**

I. Introduction

REMOTE sensing of snow cover is of primary importance for the effective management of water resources and for avalanche forecasts. The capability of passive microwave sensors to monitor seasonal variations in snow cover has been the subject of several experimental activities carried out using ground-based and satellite systems [1]–[5]. Moreover, the dielectric characteristics of several snow types have been investigated by means of experiments and theoretical models and data are currently available at frequencies up to 90 GHz [6]. Measurements carried out between 3 GHz and 90 GHz have pointed out the sensitivity of microwave emission to snow type and water equivalent. At the lower frequencies of the microwave band, emission from a layer of dry snow is mostly influenced by the soil conditions below the snow pack and by snow layering. At the higher frequencies, however, the role played by volume scattering increases, and emissivity appears sensitive to snow water equivalent (SWE) [1], [5]. If snow melts, the presence of liquid water in the surface layer determines an increase in emissivity, especially at high frequencies [6]. This is due to the transition from volume to surface scattering. The average spectra of the brightness temperature *Tb* obtained by Schanda *et al.* [7] show that the *Tb* of dry and refrozen snow decreases with frequency, whereas, the *Tb* of wet spring snow increases. In some cases, the spectral behavior of wet snow shows a slight increase with frequency due to the increasing effect of surface roughness [7].

Field measurements were carried out in March 1996 and February 1997 in the Dolomitic Alps, Italy, on various test sites at different elevations, in order to represent situations of varying snow cover conditions, including dry snow at high density with rounded polycrystals, low density fresh/dry snow and lastly a typical spring situation of wet snow with rounded particles, high surface density, and a very low consistency. On each test site, the composition of the strongly stratified snow pack was analyzed according to the standards of the International Commission on Snow and Ice [8]. Experimental data were compared with simulation results obtained using the dense medium transfer theory (DMRT). The model was found to be able to interpret experimental data.

Manuscript received December 22, 2000; revised July 16, 2001. This work was supported by the CNR-GNDCI (Gruppo Nazionale Difesa Catastrofi Idrogeologiche), PRNA (Programma Nazionale di Ricerche in Antartide), and ASI (Italian Space Agency).

The authors are with the Consiglio Nazionale delle Ricerche (CNR), Istituto di Ricerca sulle Onde Elettromagnetiche (IROE), 50127, Florence, Italy.

Publisher Item Identifier S 0196-2892(01)09283-X.

II. The Experiments

A. The Test Sites

The criterion used to select the test sites was that of having a flat surface with sufficient extension, homogeneity and free horizon, in order to guarantee the same conditions for the antenna footprints at all the observation angles. Conventional measurements included the penetration test and stratigraphic analysis. The various layers of snow were identified and the following parameters were estimated for each layer: grain shape and dimensions, density, liquid water content, temperature, and hardness [8].

The first set of measurements was carried out in March 1996 in the vicinity of Arabba. The features of snow with liquid water content changing from less than 2% to about 10% were investigated on the Rue de Mont test site, where the 50-cm-deep snowcover was typical of spring snow with melted/refrozen grains, high density (350 Kg/m^3 in the morning and 400 Kg/m^3 in the afternoon) and a uniform temperature profile close to 0 °C. During the day, the stratigraphic analysis showed a reduction in the hardness, due to the fusion process. At the Campolongo test site (1790 m a.s.l), the 67-cm-deep snowpack was characterized by a first layer (4 cm) of high hardness and high density (350 Kg/m^3), followed by intermediate layers of a low hardness composed of rounded polycrystals (2.0 mm), with small hoar crystals. The temperature profile showed a minimum (−7°C) at a depth of 40 cm and was −1°C on the surface. Said surface presented hollow furrows (3 mm). The measurements were carried out between 10:30 a.m. and 1:30 p.m. At Mount Cherz (2030 m a.s.l), the snow was 78 cm deep with low hardness and a density that ranged from 130 Kg/m^3 on the surface to 380 Kg/m^3 at the bottom. The surface layer of dry fresh snow was composed of hoar crystals and rounded small particles (1.0 mm); the air temperature during the measurements (10:30 am–1:30 pm) was −11°C. Other measurements were worked out in Falcade in February 1997. Dry snow was surveyed in two sites: a)

TABLE I
SUMMARY OF DRY SNOW CHARACTERISTICS

Site	Arabba Rue de Mont	Arabba Campolongo	Arabba Cherz	Falcade Zingari	Falcade Valles
Altitude (m)	1470	1790	2030	2150	2170
Observation date	14/3/96	11/3/96	13/3/96	20/2/97	20/2/97
Local time	11-16	12-15	10-13	9-12	13-17
air temperature (°C)	2.3	-5.5	-11.0	3.5	3
snow depth (cm) / type	50 dry/wet	67cm/dry (crust)	78 cm dry	116 cm dry	119cm dry
density profile (Kg/m^3)	unif. 350 (a.m.)/ 400(p.m)	280 (top)/ 350 (max)	130 (top) / 380(bott.)	140 (top) 400 (bott)	140 (top) 440 (bott.)
temperature profile °C (Top, -Xcm, Bottom)	uniform 0	-1 T,-7 (-40), -2 B	-8.5 T, -10 (-70), -3 B	-7 T, -2 B	-7 T, -2 B
grain size (mm) /shape	5/rounded	2-5/facets	2/stellar	2/ facets-rounded	2-3/ facets
surface hardness	very low	high	very low	medium	very low
surface roughness	convex rows (Sd)	Rows (Sc) 3mm	smooth (Sa)	smooth	smooth

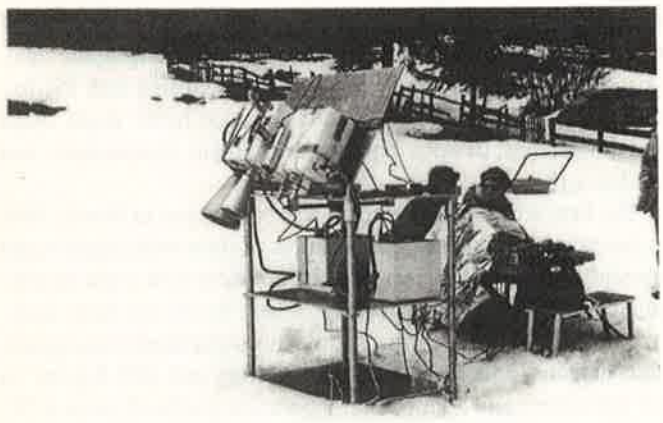

Fig. 1. Experimental equipment.

Zingari Alti (2150 m a.s.l), where the 116-cm-deep snow cover was composed mainly of angular grains or grains rounded due to the decrease in the temperature gradient. The basal layer was iced. The temperature profile had a minimum (−8.5 °C) at 100 cm and the value on the surface was −7 °C; b) Valles (2170 m a.s.l), where the snow pack (119 cm deep) was mainly composed of angular grains with an iced basal layer. A summary of snow conditions in the various test sites is provided in Table I.

B. Remote Sensing Equipment

Remote sensing data were simultaneously collected by means of a radiometer set (IROE) that measured thermal emission at three microwave frequencies: 36.5, 10.0, and 6.8 GHz and in the thermal infrared (8–14 μm) band (Fig. 1). The microwave sensors measured the horizontal and vertical polarization components of the brightness temperature at incidence angles between 30 and 60°. The instruments were portable, self-calibrated systems with a dual polarization horn antenna for each frequency channel and an internal calibration based on two loads at different temperatures (250 K ±0.2 K and 370 K ±0.2 K). The calibrated digital output signals were recorded in a notebook computer, together with the temperatures of the calibrating loads. Calibration checks in the 30 K–300 K range were carried out during the field experiments by means of absorbing panels of known emissivity and temperature (Eccosorb AN74 and VHP8) and by observing clear sky with a calibrated noise source coupled to the antenna. Background emission was periodically measured by means of a reflecting plate placed above the target and subtracted from the total emission. The measurement accuracy (repeatability achieved) was better than ±0.5 K, with an integration time of 1 s. The beamwidth of the corrugated conical horns was 20° at −3 dB and 56° −3 dB at for all frequencies and polarizations. The sensors were installed on a metal frame placed directly on the snow (Fig. 1) or on a snow cat. The observation geometry (distance between antenna and target) was arranged to meet the conditions of far field operation at an observation angle $\vartheta = 30°$ from a minimum height of 140 cm. The FOV ranged from 0.5×0.5 m^2 at an incidence angle $\vartheta = 20°$ to 5×5 m^2 at $\vartheta = 60°$. The infrared sensor, a commercial type hand-held radiometer with an accuracy (repeatability) of ±0.5 K, was placed on the same boresight as that of the microwave radiometers. Microwave emissivity was approximated by normalizing the brightness temperature to the thermometric temperature at a depth of 10 cm for measurements at 6.8 GHz and 10 GHz and to the thermometric temperature measured by infrared radiometer at 37 GHz.

III. EXPERIMENTAL RESULTS

A. Snow Type Identification

In the microwave range considered, the most suitable indexes for characterising snow covers were found to be: the normalized temperature Tn (ratio between brightness and physical temperature of snow), the microwave spectral index MSI = [Tn(37) − Tn(10)], and the polarization index PI = (Tbv − Tbh)/(Tbv + Tbh) measured at 37 GHz and $\vartheta \gtrsim 40°$. Examples of spectra of the basic types of observed surfaces (wet and dry snow) are represented in Fig. 2. We can note that the microwave spectrum shows an increase from 6.8 to 10.6 GHz for all snow types, whereas the Tn(37) − Tn(10) difference is negative on dry snow and increases as the wetness increases, up to positive values on very wet snow. It should be noted that wetness was measured according to the standard method suggested in [8]. Thus, the value is only indicative of the average value in the layer. We observe that multifrequency microwave data can be efficient in separating wet snow from dry snow on the basis of the spectral index. However, for low wetness (< 1–2%), the spectrum is very close to that of dry snow. In this case, discrimination can be better made by using the polarization index, which is much higher for dry snow (Fig. 3).

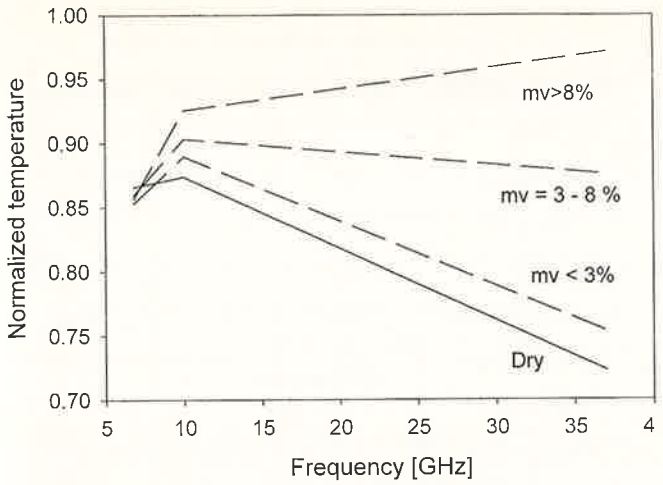

Fig. 2. Spectra of microwave normalized temperature Tn at incidence angle $\theta = 40°$ and H polarization for snow with different values of wetness estimated according to the standard method of the international commission on snow.

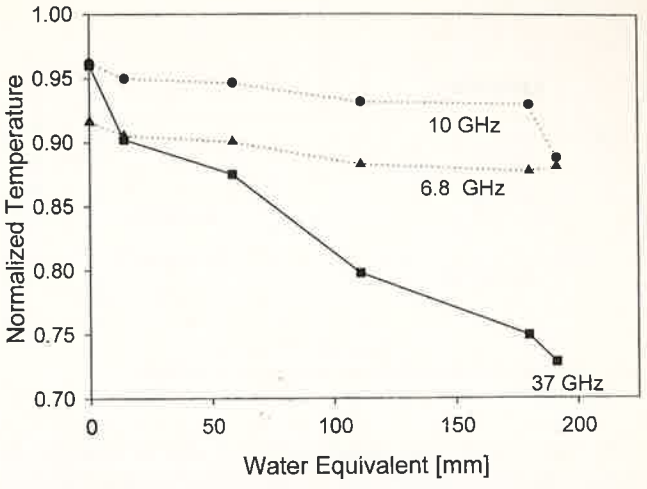

Fig. 4. Normalized temperature at 6.8, 10, and 37 GHz (at $\theta = 40°$, H polarization) as a function of the SWE.

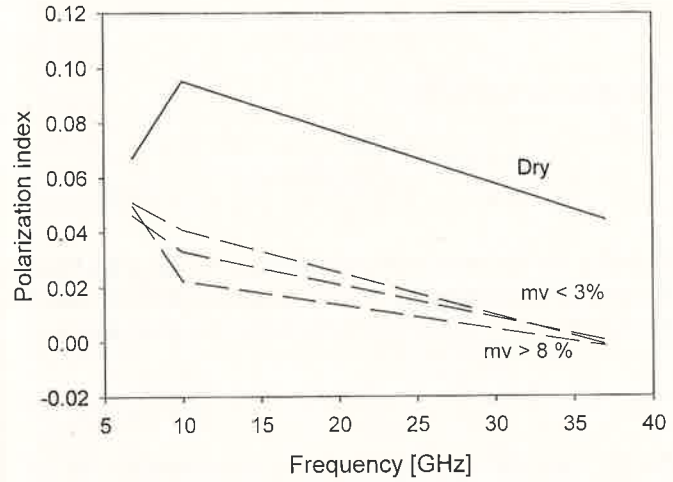

Fig. 3. Spectra of polarization index. PI = (Tbv − Tbh)/(Tbv + Tbh) measured at $\theta = 40°$ for dry and wet snow.

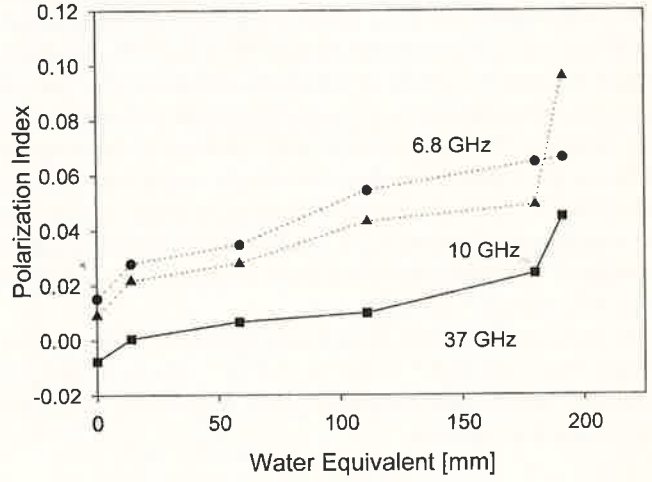

Fig. 5. Polarization index at 6.8, 10, and 37 GHz (at $\theta = 40°$) as a function of the SWE.

B. Sensitivity to Snow Depth and Water Equivalent

The characteristics of dry snow were investigated on four sites (Campolongo Pass, Mount Cherz, Valles Pass, Zingari Alti). On all these sites, the trend of normalized temperature versus incidence angle was rather flat at all frequencies, with a maximum of the polarization index at 10 GHz. To investigate the sensitivity to snow depth and SWE, measurements were carried out at Campolongo, by sequentially removing, step by step, five snow layers. The results showed that the dry snow was almost transparent at 6.8 and 10.6 GHz, whereas at 37 GHz there was a significant decrease in the brightness temperature as the snow thickness increased (Fig. 4). On the contrary, as the snow layer increased, the polarization index (PI) increased at all frequencies (Fig. 5). The sensitivity of the emission, and in particular of PI at 10 GHz, to the crust formed at the top of the snow layer is worth noting. From the diagrams of Fig. 4, we see that, as expected, the highest sensitivity to SWE was obtained at the highest frequency, and that the relationship between Tn and SWE was not a continuous function due to the changes in snow density in the various layers.

IV. The DMRT Model

For a dense medium such as snow, where particles occupy an appreciable fractional volume (more than 10% of the total volume), the assumption of independent scattering used in the conventional radiative transfer (CRT) is not valid. In this case, the brightness temperature can be computed by means of the Dense Medium Radiative Transfer Theory (DMRT), which has been derived from Dyson's equation under the quasi-crystalline approximation with coherent potential (QCA-CP) and the Bethe Salpeter equation under the ladder approximation of correlated scatterers [11], [12]. This approach takes into account the coherence of random scatterers and satisfies the energy conservation.

The mathematical form and, consequently, the numerical solutions of DMRT are the same as those for CRT, provided that three important quantities: the effective propagation constant, the extinction coefficient, and the albedo are introduced [9]. The latter quantities are computed from the permittivity of the background medium and from the particle permittivity and size distributions [9]–[11].

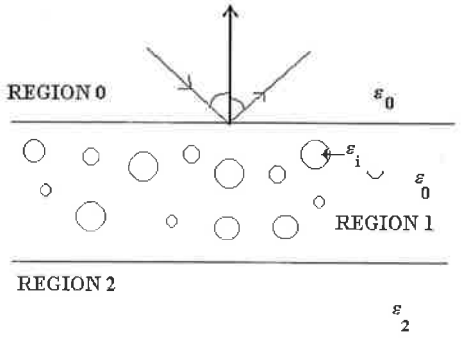

Fig. 6. Geometry of the problem for simulations with DMRT.

The snow cover was modeled from a slab of densely-distributed spherical particles with a mean radius a and permittivity $\varepsilon_s = \varepsilon_s' + i\varepsilon_s''$ embedded in a background medium of permittivity ε (air) (Fig. 6) and thickness d, overlying a homogeneous medium with a permittivity $\varepsilon_g = \varepsilon_g' + i\varepsilon_g''$. Several efforts were made to calculate an appropriate and valid pair distribution function for dry snow [12]–[15]. In this work, the correlation of particles was calculated from the Percus-Yevick (P–Y) pair distribution function g(r) [16], in which the distribution of particle sizes was described by a truncated Rayleigh probability density function. Two assumptions were inherent in deriving the effective propagation constant and albedo, using the results of the QCA-CP: 1) the particle size a had to be small compared to the wavelength of interest ($a \ll \lambda$); 2) the effective propagation constant K is assumed to have a small imaginary part compared to its real part ($K'' \ll K'$).

In accordance with the second assumption, K^2 was approximately expressed as $K^2 = K'^2 + 2iK'K''$, where K' and K'' represent the real and imaginary parts, respectively. With this approximation, we have

$$\begin{aligned} K^2 \approx & K'^2 + 2iK'K'' \\ = & K_0^2 \cdot \left\{ 1 + i\frac{2}{9}\frac{K_0 a^3 (k_s^2 - k^2)}{1 + \frac{k_s^2 - k^2}{3K_0^2}(1-f)} \frac{(1-f)^4}{(1+2f)^2} \right\}. \end{aligned} \quad (1)$$

In (1), K_0 represents the propagation constant of coherent waves in a medium where the scattering effect can be ignored. It has been shown [10], [17] that K_0 must satisfy the following equation:

$$K_0^2 = k^2 + \frac{f(k_s^2 - k^2)}{1 + \frac{k_s^2 - k^2}{3K_0^2}(1-f)} \quad (2)$$

where

k	wavenumber in background;
k_s	wavenumber in particles;
$f = n_0 4\pi a^3/3$	fractional volume occupied by particles (n_0 = number of particles per unit volume).

Mathematically, K_0 is regarded as the 0th order solution of K. K_0 is solved from (2) by using a quadratic formula.

Subsequently, $2K''$ is solved from (1) by balancing the real and imaginary parts separately.

TABLE II
SNOW PARAMETERS USED AS INPUTS FOR THE MODEL

INPUT PARAMETERS	*Campolongo*	*Zingari alti*	*Passo Valles*
Snow			
Temperature [K]	*266*	*266*	*266*
Permittivity	*3.15*	*3.15*	*3.15*
Depth [m]	*0.67*	*1.16*	*1.19*
Mean particles radius [mm]	*0.5*	*0.35*	*0.38*
Fractional volume	*0.3*	*0.3*	*0.3*
Ground			
Temperature [K]	*271*	*270*	*270*
Permittivity	*5+j 0.5*	*6+j 1.2*	*4.3+j 0.7*

The extinction rate k_e is defined as

$$k_e = 2\mathrm{Im}(K). \quad (3)$$

The albedo ω is [10], [11]

$$\omega = \frac{2}{9}\frac{a^3 f}{k_e} \left| \frac{k_s^2 - k^2}{1 + \frac{k_s^2 - k^2}{3K_0^2}(1-f)} \right|^2 \frac{(1-f)^4}{(1+2f)^2}. \quad (4)$$

Note that the last ratio in (4) was obtained by using the Percus-Yevick approximation [9], [17] in computing the pair distribution function $g(r)$, according to the following relationship

$$1 + 4\pi n_0 \int_0^\infty dr\, r^2 (g(r) - 1) = \frac{(1-f)^4}{(1+2f)^2}. \quad (5)$$

For the isotropic medium taken into consideration, we only needed to solve the VRT equation for the first two Stokes parameters I_v and I_h. In this case, we employed the Gaussian quadrature for discretizing and the discrete ordinate and eigenanalysis method for solving the equation. The integral was solved numerically as a weighted sum of N values of the integrand computed at the zeroes $\mu_i = \cos\theta_i$ of Legendre polynomials [17].

The particular solution was obtained by considering the boundary conditions, which, in this case, were

$$\overline{I}(\pi - \theta, 0) = \overline{\overline{R}}_{10} \cdot \overline{I}(\theta, 0) \quad (6)$$

$$\overline{I}(\theta, -d) = \overline{\overline{R}}_{12} \cdot \overline{I}(\pi - \theta, -d) + \overline{\overline{T}}_{21} \cdot C \cdot T_2 \quad (7)$$

where $\overline{\overline{R}}_{ij}$ and $\overline{\overline{T}}_{ij}$ are, respectively, the reflectivity and transmissivity matrices, from medium i to medium j, computed from the Fresnel relations where the permittivity of snow was obtained from the effective propagation constant $C = K'^2 K_b/(\lambda^2 k^2)$, and K_b is the Boltzman's constant. The final form of the brightness temperature observed in region 0 was [17]

$$\overline{T}_B(\theta_{i0}) = \frac{1}{C}\overline{\overline{T}}_{01}(\theta_1) \cdot \overline{I}(\theta_i, z = 0) \quad (8)$$

where $I(\theta_i, z)$ is given in [14].

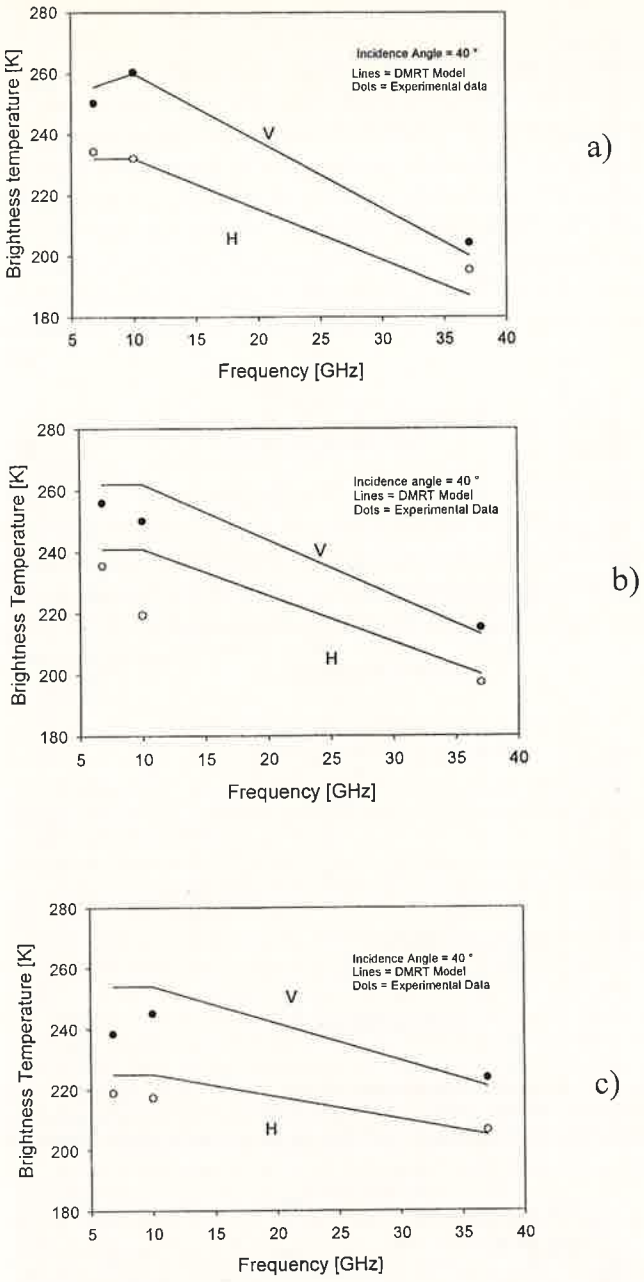

Fig. 7. Brightness temperature of dry snow versus frequency. Comparison between model simulations (DMRT) and experimental data for three test sites: (a) Campolongo, (b) Valles, and (c) Zingari Alti.

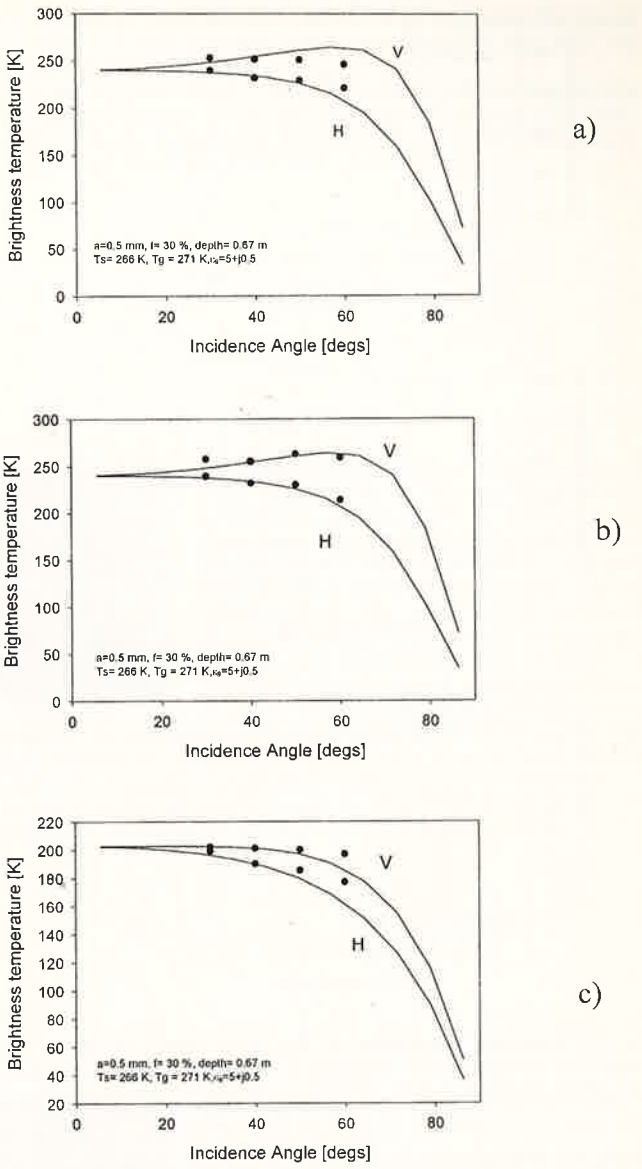

Fig. 8. Brightness temperature of dry snow versus incidence angle. Comparison between model simulations (solid line) and experimental data at (a) 6.8 GHz, (b) 10 GHz, and (c) 37 GHz for the test site located in Campolongo Pass.

V. Comparison Between Theoretical Results and Experimental Data

A comparison of model results with experimental data is performed in this section. First of all it should be noted that a major problem in using the DMRT is the discrepancy between the real and modeled shapes of ice particles. Indeed, the latter, which are of irregular shape, are approximated in the theory by spheres of radius much smaller than the wavelength. In this work, model simulations were performed by using as input parameters (fractional volume, snow depth, temperature and wetness) ground data collected simultaneously with remote sensing measurements, except for the radius of ice particles a, which was first estimated from the average volume occupied by the particles and then selected as best-fit value for experimental data at the highest frequency. Indeed, the irregular shape of the particles made it difficult to establish the radius of equivalent spheres. However, the values obtained were consistent with the estimated quantities and satisfactorily fitted experimental data at all frequencies and polarizations. The snow parameters used as inputs to the model are summarized in Table II.

The results of the comparison between theory and the experimental data collected on the test sites of Campolongo, Zingari Alti and Valles are presented in the diagrams of Figs. 7–11. The spectra of the brightness temperature (Fig. 7) show a general decrease in Tn as the frequency increases, which is typical of a medium in which scattering is dominant. However, Tb may be higher at 10 GHz than at 6.8 GHz. Also, the polarization difference is higher at X band. The trends of the brightness temperature at 6, 8, and 10 GHz and 37 GHz versus the incidence

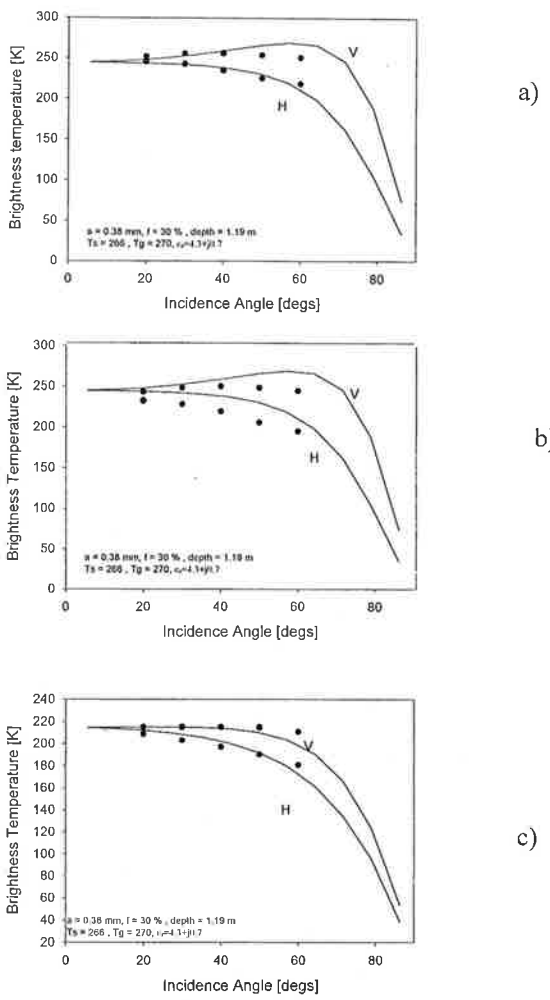

Fig. 9. Brightness temperature of dry snow versus incidence angle. Comparison between model simulations (solid line) and experimental data at (a) 6.8 GHz, (b) 10 GHz, and (c) 37 GHz for the test site located in Valles.

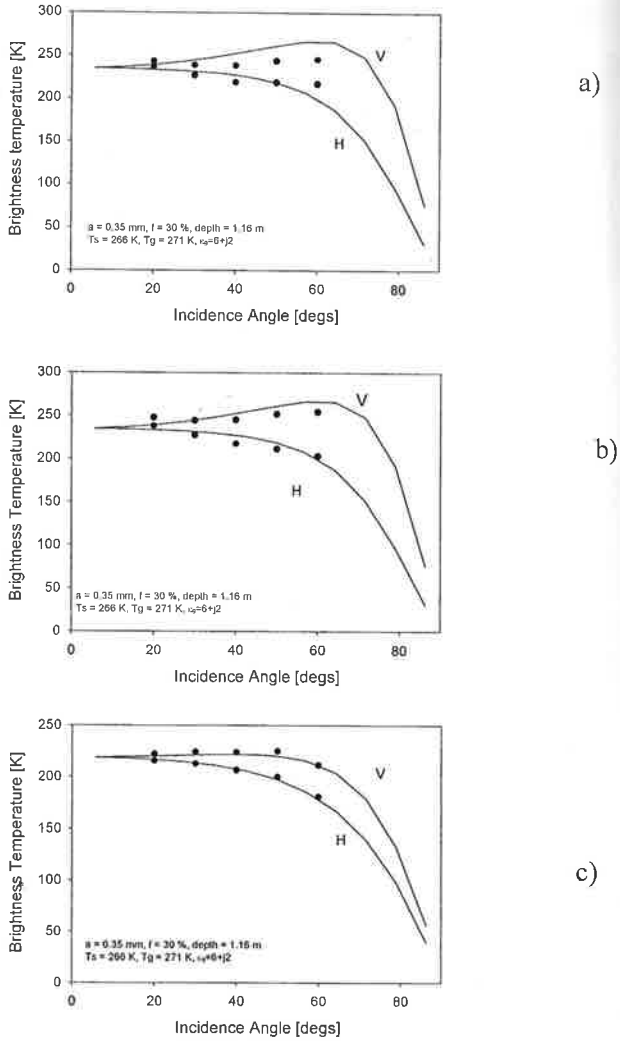

Fig. 10. Brightness temperature of dry snow versus incidence angle. Comparison between model simulations (solid line) and experimental data at (a) 6.8 GHz, (b) 10 GHz, and (c) 37 GHz for the test site located in Zingari Alti.

angle are represented in Figs. 8–10 for the three test sites of Campolongo, Valles and Zingari Alti, respectively. It should be noted that the 2–5 mm facet-like ice crystals observed at Campolongo, the 2–3 mm facets of snowpack in Valles, and the 2 mm facet-rounded particles present at Zingari Alti have been approximated by spheres that are, respectively, 1 mm, 0.7 mm, and 0.64 mm in diameter. Finally, the relationship between the brightness temperature and the SWE for data, collected at Campolongo at 10 and 37 GHz for an incidence angle $\theta = 40°$, is shown in Fig. 11. The SWE defined as

$$W = \int_0^d \rho \, dz$$

was computed by discretizing the integral, i.e.,

$$W \cong \sum_1^{10} \rho_i \Delta z_i \tag{9}$$

where the snow density ρ_i of the stratified snow pack was measured in ten significant layers of thickness Δz_i.

Since the snow density in the vertical profile changed from 280 to 350 Kg/m^3, in the model, we adopted the same weighted

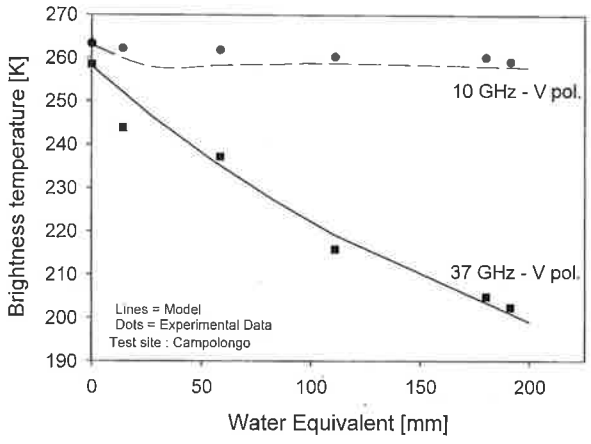

Fig. 11. Brightness temperature measured at $\theta = 40°$ incidence angle as a function SWE. Comparison between experimental and model results.

average value used in the simulations of angular trends of Tb. The model confirmed that the brightness temperature at 37 GHz is sensitive to SWE, whereas this sensitivity is weak at 10 GHz.

VI. Concluding Remarks

Experimental data on microwave emission from dry snow collected on the Italian Alps have been compared with theoretical simulations performed with the DMRT. Model inputs were obtained from nivological measurements carried out using standard methods and an electromagnetic contact probe. The results obtained demonstrated the capability of the DMRT to represent experimental data. It was shown that a dual-frequency microwave radiometer is able to separate dry snow from wet snow and that the microwave emission at 37 GHz is sensitive to the SWE.

Acknowledgment

The authors wish to thank A. Cagnati, M. Valt, and R. Zasso of CSVDI, Arabba, Italy, who carried out the nivological measurements, and the "Società Falcade" for its kind collaboration in the measurements taken in Falcade. They would also like to thank Prof. Y. Q. Jin for reading the manuscript and making very helpful suggestions.

References

[1] R. Hofer and C. Mätzler, "Investigation of snow parameters by radiometry in the 3- to 60-mm wavelength region," *J. Geophys. Res.*, vol. 85, pp. 453–460, 1980.

[2] W. H. Stiles and F. T. Ulaby, "The active and passive microwave response to snow parameters, 1: Wetness," *J. Geophys. Res.*, vol. 85, pp. 1037–1059, 1980.

[3] ——, "The active and passive microwave response to snow parameters, 2: Water equivalent," *J. Geophys. Res.*, vol. 85, pp. 10 457–11 049, 1980.

[4] C. Mätzler, H. Schanda, and W. Good, "Toward the definition of optimum sensor specification for microwave remote sensing of snow," *IEEE Trans Geosci. Remote Sensing*, vol. GE-20, pp. 57–66, Jan. 1982.

[5] H. Rott and K. Sturm, "Microwave signature measurements of Antarctic and Alpine snow," in *Proc. 11th EARSeL Symp.*, Graz, Austria, 1991, pp. 140–151.

[6] M. T. Hallikainen, F. T. Ulaby, and T. E. Van Deventer, "Extinction behavior of dry snow in the 18–90 GHz range," *IEEE Trans Geosci. Remote Sensing*, vol. GE-25, pp. 737–745, 1987.

[7] E. Schanda, C. Mätzler, and K. Künzi, "Microwave remote sensing of snow cover," *Int. J. Remote Sensing*, vol. 4, pp. 149–158, 1983.

[8] S. Colbeck, E. Akitaya, R. Armstrong, H. Gubler, J. Lafeuille, K. Lied, D. McClung, and E. Morris, "The International Classification for Seasonal Snow on the Ground," Int. Commission Snow Ice Rep., IAHS, 1993.

[9] Y.-Q. Jin, *Electromagnetic Scattering Modeling for Quantitative Remote Sensing*. Singapore: World Scientific, 1993.

[10] R. West, L. Tsang, and D. P. Winebbrenner, "Dense medium radiative transfer theory for two scattering layers with a Rayleigh distribution of particle sizes," *EEE Trans. Geosci. Remote Sensing*, vol. 31, pp. 426–437, Mar. 1993.

[11] L. Tsang and J. Kong, "Scattering of electromagnetic waves from a half space of densely distributed dielectric scatterers," *Radio Sci.*, vol. 18, pp. 1260–1272, 1983.

[12] P. R. Siqeuira, K. Sarabandi, and F. T. Ulaby, "Numerical simulation of scatterer positions in a very dense medium with an application to the two-dimensional born approximation," *Radio Sci.*, vol. 30, pp. 1325–1339, Sept.–Oct. 1995.

[13] L. M. Zurk, L. Tsang, J. Shi, and R. E. Davis, "Electromagnetic scattering calculated from pair distribution functions retrieved from planar snow sections," *IEEE Trans. Geosci. Remote Sensing*, vol. 35, pp. 1419–1428, Nov. 1997.

[14] K. H. Ding, L. M. Zurk, and L. Tsang, "Pair distribution functions and attenuation rates for sticky particles in dense media," *J. Electromagn. Waves Applicat.*, vol. 8, pp. 1585–1604, Dec. 1994.

[15] C. Mätzler, "Autocorrelation functions of granular media with free arrangement of spheres, spherical shells or ellipsoids," *J. Appl. Phys.*, vol. 81, pp. 1509–1517, Feb. 1997.

[16] J. Percus and G. Yevick, "Analysis of classical statistical mechanics by means of collective coordinates," *Phys. Rev.*, vol. 110, pp. 1–13, 1958.

[17] L. Tsang, J. A. Kong, and R. T. Shin, *Theory of Microwave Remote Sensing*. New York: Wiley, 1985.

Giovanni Macelloni was born in Florence, Italy, in 1966. He received the Dr. Eng. degree from the University of Florence, Florence, Italy, in 1993.

He joined the Institute of Research of Electromagnetic Waves, National Council of Research, Florence, Italy, in 1993. His research interests include passive and active microwave remote sensing of soil, vegetation, and snow, using satellite, airborne, and ground-based data. His research also deals with development of passive and active microwave modeling and development of microwave radiometers. He had participated in various international remote sensing campaigns (NOPEX 95, STAAARTE—RESEDA 97, STAAARTE—FORMON 99, MAP-99), where he was responsible for IROE microwave radiometers.

Dr. Macelloni has served as a reviewer for several international journals, including IEEE Transactions on Geoscience and Remote Sensing.

Simonetta Paloscia received the degree in agricultural sciences from the University of Florence, Florence, Italy, in 1979.

In 1979, she joined the National Research Council (CNR), IATA, Florence, Italy, where she worked in agrometeorology and remote sensing studies concerning agricultural crops. Since 1987, she has been with the Institute of Reasearch on Electromagnetic Waves (IROE), CNR, where she has continued studying natural surfaces using microwave and infrared remote sensing techniques. Her current research concerns microwave remote sensing of land and in particular, the study of relationships between microwave emission and backscattering and plant and soil biophysical parameters. She has been a Visiting Scientist with the Institute of Radio Engineering of Moscow (URSS), Moscow, Russia, the Institute for Remote Sensing Applications, China, and the Massachusettts Institute of Technology (MIT), Cambridge. She had participated in various microwave remote sensing campaigns (SAR-580, AGRISAR, AGRISCATT'87, AGRISCATT'88, MAC'91, and SIR-C/X-SAR), where she has coordinated the activities of ground truth data collection. She is Co-Investigator of the SIR-C/X-SAR and ERS-1/2/3 Projects, and was Principal Investigator of the JERS-1 Project. She collaborates with the Department of Earth Sciences, University of Florence, Florence, Italy, for a research activity on soil erosion using SAR images. Since 1996, she has been a Member of the NASDA ADEOS II-AMSR Science Team for land applications. She has published over 80 papers on International Journal and Conference Proceedings and has edited a book with VSP Press (The Netherlands).

Dr. Paloscia has served as Chairman of the 6th Specialist Meetings on Microwave Radiometry and Remote Sensing, Florence, Italy, 1999, and as reviewer for many international journals. She is a member of the Electromagnetic Academy (USA), and an affiliate member of the IEEE Geoscience and Remote Sensing Society.

Paolo Pampaloni (M'86–SM'95–F'99) is Head of the Remote Sensing Department, the Institute of Research on Electromagnetic Waves (IROE), Italian National Research Council (CNR), Florence, Italy. He has been a Consultant with the European Space Agency, Paris, France, for microwave radiometry as a member of several scientific advisory groups and committees. He has served as Principal Investigator and Co-Investigator of many international projects and experiments in Europe and as X-SAR/SIR-C Project Scientist. He has been a Visiting Scientist with the Institute of Radio Engineering of Moscow (URSS), Moscow, Russia, the Institute for Remote Sensing Applications, China, and the Massachusettts Institute of Technology (MIT), Cambridge. He has published over 100 papers on International Journal and Conference Proceedings and has edited three books with VSP Press (The Netherlands). His current research deals with active and passive microwave remote sensing of the environment and in particular with the study of microwave emission and scattering from natural media.

Dr. Pampaloni has served as General Chairman of the *2nd Specialist Meetings on Microwave Radiometry and Remote Sensing*, Florence, 1988, and *6th Specialist Meetings on Microwave Radiometry and Remote Sensing*, Florence, 1999, and of IGARSS'95. He is an Associate Editor of IEEE TRANSACTIONS ON GEOSCIENCE AND REMOTE SENSING and has served as Reviewer for many international journals. He is a member of Electromagnetic Academy (USA) and President of the Center for Microwave Remote Sensing.

Marco Tedesco was born in Naples, Italy, in 1971. He received the Electronic Engineering Degree from the University of Naples "Federico II", Naples, Italy in 1999 with the thesis 'Microwave employment for woodworm destruction: numerical analysis and experimental validations'. In 1999 he joined the Institute of Research on Electromagnetic Waves (IROE) of the Italian National Research Council (CNR). He is now a Ph.D. student at IROE. His research interests include passive and active microwave remote sensing of snow, development of microwave modeling, numerical simulations and inverse problems.